Finite Dimensional Approximation to Muscular Response in Force-Fatigue Dynamics using Functional Electrical Stimulation

Toufik Bakir, Bernard Bonnard, Sandrine Gayrard, Jérémy Rouot

Finite Dimensional Approximation to Muscular Response in Force-Fatigue Dynamics using Functional Electrical Stimulation

Toufik Bakir [a], Bernard Bonnard [b,c], Sandrine Gayrard [a,c], Jérémy Rouot [d]

[a] *Univ. Bourgogne Franche-Comté, ImViA Laboratory EA 7508, 9 avenue Alain Savary, Dijon, France*

[b] *Univ. Bourgogne Franche-Comté, Institut de Mathématiques de Bourgogne, Unité CNRS UMR 5584, Dijon, France, 9 avenue Alain Savary, Dijon, France*

[c] *INRIA, 2004 Route des Lucioles, 06902 Valbonne, France*

[d] *Univ. Brest, UMR CNRS 6205, Laboratoire de Mathématiques de Bretagne Atlantique 6, Avenue Victor Le Gorgeu, 29200 Brest, France*

Abstract

Recent dynamical models, based on the seminal work of V. Hill, allow to predict the muscular response to functional electrostimulation (FES), in the isometric and non-isometric cases. The physical controls are modeled as Dirac pulses and lead to a sampled-data control system, sampling corresponding to times of the stimulation, where the output is the muscular force response. Such a dynamics is suitable to compute optimized controls aiming to produce a constant force or force strengthening, but is complex for real time applications. The objective of this article is to construct a finite dimensional approximation of this response to provide fast optimizing schemes for the design of a smart electrostimulator for muscular reinforcement or rehabilitation. It is an on-going industrial project based on force-fatigue models, validated by experiments. Moreover it opens the road to application of optimal control to track a reference trajectory in the joint angular variable to produce movement in the non-isometric models.

Key words: Biomechanics · Force-fatigue models · Sampled-data control · Nonlinear input-output approximation · Predictive-correction methods in optimization.

1 Introduction

Based on the seminal work of V. Hill depicted in Gesztelyi et al. (2012), recent mathematical models (experimentally validated) allow to predict the force response to external stimulation. They are presented and discussed in details in Wilson (2011) in the non-fatigue isometric case. They were extended in particular by Ding et al. (2000, 2002a,b) to take into account the muscular fatigue due to a long stimulation period and later in Marion et al. (2013) to analyze the joint angular variable response in the non-isometric case aiming to produce movements. Such models contain two basic nonlinearities and constitute the intricate part of the dynamics. First of all, the ionic conduction and the nonlinear effect of successive pulses on the Ca^{2+}-concentration. Second, the nonlinear dynamics relating the muscular force response to such concentration, modeled by the Michaelis-Menten-Hill functions, see Michaelis et al. (1913).

For each train of pulses, due to digital constraints, only a finite number of pulses can be applied and from the optimal control point of view, the problem fits into the frame of optimal sampled-data control problems, studied in particular in Bourdin et al. (2016) to derive Pontryagin necessary conditions. They can be analyzed to

⋆ This paper was not presented at any IFAC meeting. It benefited from the support of the FMJH Program PGMO and from the support of EDF; Thales, Orange and the authors are partially supported by the Labex AMIES. Corresponding author J. Rouot. Email. jeremy.rouot@univ-brest.fr.

Email addresses: toufik.bakir@u-bourgogne.fr (Toufik Bakir), bernard.bonnard@u-bourgogne.fr (Bernard Bonnard), sandrine.gayrard@grenoble-inp.org (Sandrine Gayrard), jeremy.rouot@univ-brest.fr (Jérémy Rouot).

determine optimized train pulses and compared with direct optimizing schemes. A previous series of articles described the optimal control problems related to track a reference force or force strengthening, the control being either the interpulse $I_i = t_i - t_{i-1}$ between two successive pulses or the amplitude of each pulse. In particular, a model predictive control (MPC) method is presented in Bakir et al. (2019) and is based on online optimized closed loop control using a force-fatigue model, as suggested in Doll et al. (2015). Direct methods vs indirect methods based on Pontryagin type necessary conditions are discussed and numerically implemented in Bakir et al. (2020) for the isometric case and in Bonnard et al. (2020) for the non-isometric case.

The conclusion of aforementioned articles is that the nonlinear dynamics is computationally expensive due to the numerical integration procedure and a challenging task is to reduce this time for real time computation in the applications. This article is motivated by the design of a smart electrostimulator, where the Ding et al. model is used to adjust automatically the frequency and the amplitude of the stimulations and to compute the sequence of stimulations and rest periods adapted to the task of the training program, e.g. endurance program or force strengthening program. The objective of this article being to bypass the computational difficulty by constructing a finite dimensional approximation of the force response, depending upon the parameters of each individual, which can be online estimated, aiming a real time computation of the optimized amplitudes and impulse times. Note that this approximation has been coded and the application scheme to the smart electrostimulator is briefly presented in the final section.

The article is organized as follows. In section 2, the mathematical model called the Ding et al. model presented by Ding et al. (2000, 2002a,b) is introduced and the main properties of the dynamics are described, reflecting the features of the muscular activity. Hence our analysis can be applied to different models discussed in Wilson (2011). The section 3 presents the optimization problems, in relation with muscular dynamics and oriented towards the design of a smart electrostimulator, where each training program must be translated into an optimization problem. Section 4 is the technical contribution of this article, that is the construction of the approximation for real time computation. In section 5, we present some numerical simulations to validate the approximation and the optimizing scheme. In the final section 6, we outline the application to the design of the smart electrostimulator. It is based on a nonlinear output tracking, see Hirschorn et al. (1987, 1988); Isidori (1995) as a general theoretical frame, and is applied to produce a constant force in our situation, but it can be extended to the non-isometric case to obtain any reference force. The conclusion indicates directions to complete our analysis, related to online parameters estimation of the problems Stein et al. (2013); Wilson (2011) and MPC-methods presented in Richalet (1993); Wang et al. (2010) suitable for practical applications.

2 Force-fatigue model

We present the Ding et al. force-fatigue model Ding et al. (2000, 2002a,b), extension of the original Hill model Gesztelyi et al. (2012).

2.1 Ding et al. force fatigue model.

The FES input over a pulse train $[0, T]$ is the signal

$$t \mapsto \sum_{i=0}^{n} \eta_i \delta(t - t_i), \quad t \in [0, T], \tag{1}$$

where $0 = t_0 < t_1 < \cdots < t_n < t_{n+1} = T$ are the impulsion times with $n \in \mathbb{N}$ being fixed, η_i being the amplitudes of each pulses, which are convexified by taking $\eta_i \in [0, 1]$ and $\delta(. - t_i)$ denoting the Dirac (generalized) function at time t_i.

Such physical control provides the FES-signal

$$E(t) = \frac{1}{\tau_c} \sum_{i=0}^{n} R_i e^{-\frac{t-t_i}{\tau_c}} \eta_i H(t - t_i),$$

where H is the Heaviside function. E depends upon the time response parameter τ_c and the scaling function R_i is defined, given a fatigue parameter $\overline{R}$, by

$$R_i = \begin{cases} 1 & \text{if } i = 0 \\ 1 + (\overline{R} - 1)\, e^{-(t_i - t_{i-1})/\tau_c} & \text{for } i = 1, \ldots, n, \end{cases}$$

which codes the memory effect of successive muscle contractions and is associated to *tetanus* Wilson (2011).

The FES signal drives the evolution of the electrical conduction describing the evolution of Ca^{2+}-concentration c_N, which is related to the force F and the fatigue variables (A, K_m, τ_1) through the *Michaelis-Menten-Hill functions* introduced in Michaelis et al. (1913) and defined by

$$m_1(t) = \frac{c_N(t)}{K_m(t) + c_N(t)}, \; m_2(t) = \frac{1}{\tau_1(t) + \tau_2\, m_1(t)}. \tag{2}$$

The time evolution of these variables is governed by the Ding et al. force-fatigue model

$$\dot{c}_N(t) = E(t) - \frac{c_N(t)}{\tau_c}, \tag{3}$$

$$\dot{F}(t) = -m_2(t)\, F(t) + m_1(t) A(t), \tag{4}$$

$$\dot{A}(t) = -\frac{A(t) - A_0}{\tau_{fat}} + \alpha_A\, F(t), \tag{5}$$

$$\dot{K}_m(t) = -\frac{K_m(t) - K_{m,0}}{\tau_{fat}} + \alpha_{K_m} F(t), \tag{6}$$

$$\dot{\tau}_1(t) = -\frac{\tau_1(t) - \tau_{1,0}}{\tau_{fat}} + \alpha_{\tau_1} F(t), \tag{7}$$

where typical parameters values are reported in Table 1.

2.2 Non-fatigue model.

The variables $\xi_1(t) = \alpha_{K_m}(A(t) - A_0) - \alpha_A(K_m(t) - K_{m,0})$ and $\xi_2(t) = \alpha_{\tau_1}(A(t) - A_0) - \alpha_A(\tau_1(t) - \tau_{1,0})$ satisfy the linear differential equations

$$\dot{\xi}_i(t) = -\frac{1}{\tau_{fat}}\,\xi_i(t),\ i = 1, 2,$$

and we obtain an explicit expression of $K_m(t)$ and $\tau_1(t)$ as soon as $A(t)$ is explicit. Moreover, the fatigue dynamics (5) is linear and can be integrated explicitly once F – or its approximation – is fixed in some appropriate category of functions. This is the purpose of Section 4 to provide such category in which an approximation of F is derived.

Therefore, the intricate part of model (3)-(7) consists of the nonlinear force dynamics (4), which is related to the historical Hill model recollected by Gesztelyi et al. (2012) and we shall restrict our mathematical analysis to the case where the fatigue variables (A, K_m, τ_1) have constant dynamics (non-fatigue model).

The concentration $c_N(\cdot)$ can be written explicitly as

$$c_N(t) = \frac{1}{\tau_c}\sum_{i=0}^{n} R_i\eta_i(t - t_i)\, e^{-\frac{t-t_i}{\tau_c}}\, H(t - t_i), \tag{8}$$

and the model considered in this paper consists of the nonlinear *non-fatigue model*

$$\dot{F}(t) = -m_2(t)\, F(t) + m_1(t)A, \tag{9}$$

where the fatigue variables $(A(\cdot), K_m(\cdot), \tau_1(\cdot)) \equiv (A_0, K_{m,0}, \tau_{1,0})$ are constant (see Table 1).

This restriction to a simpler model is not a limiting aspect of the method presented in Section 4, which can be adapted to various models derived from the Ding et al. model, in particular in the nonisometric case Marion et al. (2013). More generally, we believe that our method is suitable for models arising from a sampled-data control framework but this generalization is not the purpose of this article.

Sampled-data control system. Writing E as

$$E(t) = \frac{e^{-t/\tau_c}}{\tau_c}\ \sum_{i=0}^{n} \underbrace{R_i\eta_i e^{-t_i/\tau_c}\, H(t - t_i)}_{u_i(t)},$$

the *non-fatigue model* can be formulated as

$$\dot{x}(t) = g(x(t)) + \frac{e^{-t/\tau_c}}{\tau_c}\ \sum_{i=0}^{n} u_i(t)\, \boldsymbol{e}, \tag{10}$$

where $x = (c_N, F)$, g is defined from (3) and (9), $\boldsymbol{e} = (1, 0)^\intercal$ and $u_i(t)$ is the effect of the pulse and is constant over each interval $[t_i, t_{i+1}]$, $i = 0, \ldots, n$.

Observe that each impulse has an effect on the whole train $[0, T]$. We come accross a sampled-data control problem defined below.

Definition 1 *Consider a control system of the form: $\frac{\mathrm{d}x}{\mathrm{d}t} = f(x, u)$ where $x \in \mathbb{R}^d$, $u \in U \subset \mathbb{R}^m$. It is said permanent if u is a measurable bounded mapping valued in U. It is called a sampled-data control system if the set of controls is restricted to the set of piecewise constant mappings $[u_0, u_1, \ldots, u_n]$, $u_i \in U$ over a set of times $t_0 = 0 < t_1 < \cdots < t_n < T = t_{n+1}$, where n is a fixed integer.*

Input-Output mapping. The variable $\sigma = (t_1, \ldots, t_n, \eta_0, \eta_1, \ldots, \eta_n)$ belongs to the finite dimensional input-space $\mathcal{I} \subset [0, T]^n \times [0, 1]^{n+1}$ defined by the constraints

$$\begin{aligned} &0 \le \eta_i \le 1,\ i = 0, \ldots, n,\\ &t_0 = 0 < t_1 < \cdots < t_n < t_{n+1} = T,\\ &t_i - t_{i-1} \ge I_{\min},\quad i = 1, \ldots, n\ , \end{aligned}$$

where $I_{\min}$ is the smallest admissible interpulse.

The control system is observed using the following observation function

$$y(t; \sigma) = h(x(t; \sigma)), \tag{11}$$

and $h : x \mapsto F$ serves as a direct measure of the muscular force, where to emphasize the dependence of a function, say ψ, with respect to some parameters γ, we use the notation $\psi(\cdot; \gamma)$.

We derive an important regularity property of the input-output function, which is the object of study of this article.
Integrating (9), the force with $F(0) = 0$ can be written for $t \in [0, T]$ as

$$F(t; \sigma) = A_0 M(t; \sigma) \int_0^t M^{-1}(s; \sigma) m_1(s; \sigma)\, \mathrm{d}s, \tag{12}$$

Table 1
List of variables and values of the constant parameters in the Ding et al. model

Symbol	Unit	Value	Description
C_N	—	—	Normalized amount of Ca^{2+}-troponin complex
F	kN	—	Force generated by muscle
t_i	s	—	Time of the i^{th} pulse
n	—	—	Total number of the pulses before time t
i	—	—	Stimulation pulse index
τ_c	s	0.02	Time constant that commands the rise and the decay of C_N
R	—	1.143	Term of the enhancement in C_N from successive stimuli
A	$\frac{\text{mN}}{s}$	—	Scaling factor for the force and the shortening velocity of muscle
τ_1	s	—	Force decline time constant when strongly bound cross-bridges absent
τ_2	s	0.1244	Force decline time constant due to friction between actin and myosin
K_m	—	—	Sensitivity of strongly bound cross-bridges to C_N
A_0	$\frac{\text{mN}}{s}$	3.009	Value of the parameter A when muscle is not fatigued
$K_{m,0}$	—	0.103	Value of the parameter K_m when muscle is not fatigued
$\tau_{1,0}$	s	0.05095	The value of the parameter τ_1 when muscle is not fatigued
α_A	$\frac{1}{s^2}$	$-4.0\ 10^{-1}$	Coefficient for the force-model parameter A in the fatigue model
α_{K_m}	$\frac{1}{s\cdot\text{mN}}$	$1.9\ 10^{-2}$	Coefficient for the force-model parameter K_m in the fatigue model
α_{τ_1}	$\frac{1}{\text{mN}}$	$2.1\ 10^{-2}$	Coefficient for force-model parameter τ_1 in the fatigue model
τ_{fat}	s	127	Time constant controlling the recovery of $(A,\ K_m,\ \tau_1)$

where $M(t;\sigma) = \exp\left(-\int_0^t m_2(s;\sigma)\,\mathrm{d}s\right)$.

Since c_N is a (piecewise) sum of products of polynomial and exponential functions with respect to σ (see (8)), the function $\sigma \mapsto M^{-1}(s;\sigma)m_1(s;\sigma)$ is a (piecewise) sum of rational products of polynomial and exponential functions on $[0,T]$. Their partial derivatives with respect to η_i, t_i exist and are continuous on $\mathcal{I}$ (bounded) for almost every $s \in (0,T)$. According to the regularity of an integral involving parameters (Ambrosio et al., 2011, Appendix A), $\sigma \mapsto F(t;\sigma)$ has continuous differential, and we deduce the following proposition.

Proposition 2 *The input-output mapping $\sigma \mapsto y(t;\sigma)$ is differentiable with continuous partial derivatives on $\mathcal{I}$.*

3 Optimization problems related to the design of the electrostimulator

3.1 Standard electrostimulators vs smart electrostimulators

The standard commercial electrostimulators apply a sequence of pulses trains and rest periods, where on each train $[0,T]$ the user only imposes the amplitude of the pulses trains and the frequency is related to the training program, typically low frequency for endurance program and high frequency for force strengthening program. Our aim is to introduce optimization problems related to the design of a smart electrostimulator, which will be discussed in Section 6.

3.2 Optimization problems

3.2.1 The punch program

In this case, we wish to optimize the force at the end of the train over each train $[0,T]$. This leads to:

OCP1: $\max_\sigma F(T)$.
The amplitudes can be held at the constant maximal values $\eta_i = 1,\ i = 0,\dots,n$ and the optimization variables are the impulse times:

$$0 = t_0 < t_1 < \cdots < t_n < T.$$

Since one considers a single train, the force model is sufficient.

3.2.2 The train endurance program

We consider a single train $[0,T]$ on which the model is the force model and the corresponding problem is

OCP2: $\min_\sigma \int_0^T |F(t) - F_{ref}|^2\,\mathrm{d}t$.

Here, the amplitudes are appended to the impulse times to form the optimization variables and we use the convexified amplitudes constraints: $\eta_i \in [0,1],\ i = 0,\dots,n$.

The reference force has to be adjusted in relation with the user and can be set to $F_{\max}/\rho$, where ρ is a suitable positive number greater than 1 and $F_{\max}$ is deduced from **OCP1**.

4 Construction of an integrable model for real time application

4.1 Mathematical analysis of c_N

The response c_N to a pulses train $\sigma = (t_1,\dots,t_n,\eta_0,\dots,\eta_n)$, given by (8), is a sum of lobes

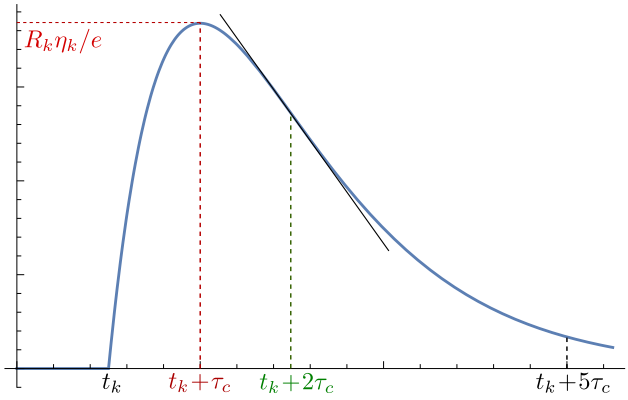

Fig. 1. The lobe ℓ_k (see (13)) reaches its maximum at $t = t_k+\tau_c$ and is equal to $R_k\eta_k/e$. It is zero for $t \le t_k$, strictly increasing on $[t_k, t_k+\tau_c]$ and strictly decreasing $[t_k+\tau_c, T]$. ℓ_k is concave on $[t_k, t_k+2\tau_c]$ and convex on $[t_k+2\tau_c, T]$. For all $t \ge t_k+5\tau_c$, $|\ell_k(t)| \le \overline{R}\,5e^{-5} \le 3.4\%\overline{R}$.

$\ell_k,\ k = 0, \dots, n$ defined as

$$\ell_k(t) \coloneqq R_k\eta_k \frac{t-t_k}{\tau_c} e^{-(t-t_k)/\tau_c} H(t-t_k). \tag{13}$$

The mathematical properties of a lobe are outlined in Fig.1.

Notation. Throughout the paper, the notation g^k refers to the restriction of a function $g : [0,T] \to \mathbb{R}$ on $[t_k, t_{k+1}]$ and $\overline{g}^k$ refers to the average of g^k on $[t_k, t_{k+1}]$.

Computing, we have

$$c_N^k(t) = \sum_{i=0}^{k} R_i\eta_i \frac{t-t_i}{\tau_c} e^{-(t-t_i)/\tau_c}. \tag{14}$$

4.2 Approximation of Michaelis-Menten-Hill functions.

For $k \in \{0, \dots, n\}$, we have $\dot{m}_1 = K_m\dot{c}_N/(K_m+c_N)^2$ and $\dot{m}_2 = \tau_2\dot{m}_1/(\tau_1+\tau_2 m_1)^2$, therefore m_1^k (resp. m_2^k) is maximal (resp. minimal) when c_N^k is maximal, that is at time

$$t_k^* \coloneqq \underset{t\in[t_k,t_{k+1}]}{\operatorname{argmax}}\ c_N^k(t)$$

and, from (14), we get

$$t_k^* = \tau_c + \frac{\sum_{i=0}^{k} R_i\eta_i\, t_i\, e^{t_i/\tau_c}}{\sum_{i=0}^{k} R_i\eta_i\, e^{t_i/\tau_c}} \le t_k+\tau_c. \tag{15}$$

In the rest of the paper, we assume that $(\eta_0, \dots, \eta_n)$ is a nonzero vector and $I_{\min} \ge \tau_c$ to ensure that $t_{k+1} \ge t_k+\tau_c \ge t_k^*$.

It follows that m_1^k (resp. m_2^k) is strictly increasing (resp. decreasing) on $[t_k, t_k^*]$ and strictly decreasing (resp. increasing) of $[t_k^*, t_{k+1}]$.

Computing, we have

$$\ddot{m}_1^k = \frac{K_m}{(K_m+c_N^k)^2}\left(\ddot{c}_N^k - \frac{2\dot{c}_N^{k\,2}}{K_m+c_N^k}\right)$$

and

$$\ddot{c}_N^k(t) = \sum_{i=0}^{k} \frac{R_i\eta_i}{\tau_c^2}\left(\frac{t-t_i}{\tau_c} - 2\right) e^{-(t-t_i)/\tau_c}.$$

Hence, we draw:

$$\begin{aligned}\ddot{c}_N^k(t) \le 0 &\Leftrightarrow \sum_{i=0}^{k} R_i\eta_i(t-t_i-2\tau_c)e^{t_i/\tau_c} \le 0\\ &\Leftrightarrow t \le t_k^*+\tau_c\end{aligned}$$

and m_1^k is concave on $[t_k, \min(t_k^*+\tau_c, t_{k+1})]$. Likewise,

$$\ddot{m}_2^k = -\frac{A_0\tau_2}{(\tau_1+\tau_2 m_1^k)^2}\left(\ddot{m}_1^k - \frac{2\tau_2\dot{m}_1^{k\,2}}{\tau_1+\tau_2 m_1^k}\right)$$

and m_2^k is convex on $[t_k, \min(t_k^*+\tau_c, t_{k+1})]$.

We define the category of functions in which we will construct the approximation of the input-output mapping.

Definition 3 *A function $f : [0,T] \to \mathbb{R}$ is in the (piecewise smooth) polynomial-exponential category $\mathcal{C}_{pe}$ if f can be expressed on each interval $[t_k, t_{k+1}]$ as sums of products of polynomials P_i and exponential terms : for $t \in [t_k, t_{k+1}]$, $f^k(t) = \sum_i P_i(t)e^{\lambda_i t},\ \lambda_i \in \mathbb{R}$.*

The category $\mathcal{C}_{pe}$ is stable with respect to integration and derivation. The c_N function is in $\mathcal{C}_{pe}$ but m_1, m_2, F do not.

An important question is to determine the "best category" of functions we should use to construct approximations of m_1, m_2, F. Since the functions m_1, m_2 are (piecewise) concave and convex respectively, it is natural to compute (piecewise) polynomial approximations $\widetilde{m}_1, \widetilde{m}_2$ as follows.

We consider a finer partition of $(t_i)_{1\le i\le n}$ denoted as $(t_{i+j/p})_{0\le i\le n,\, 0\le j\le p-1}$, $p \in \mathbb{N}^*$, such that it satisfies $t_i < t_{i+1/p} < \cdots < t_{i+(p-1)/p} < t_{i+1}$.

The approximation of m_1, m_2 goes as follows. For simplicity, we present the construction on a specific example used for the numerical simulations in Section 5. We choose $p = 2$ and on $[t_{k+j/2}, t_{k+(j+1)/2}]$, $j = 0, 1$, the

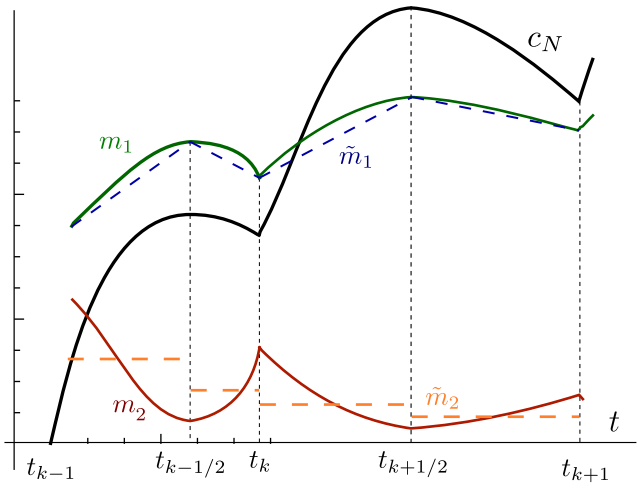

Fig. 2. Construction of the approximation $\widetilde{m}_1$, $\widetilde{m}_2$ of the Michaelis-Menten-Hill functions.

functions m_1, m_2, are approximated by the piecewise affine functions:

$$\widetilde{m}_1^k(t) = a_{j,k}\,(t - t_{k+j/2}) + b_{j,k},$$
$$\widetilde{m}_2^k(t) = \frac{m_2(t_{k+j/2}) + m_2(t_{k+(j+1)/2})}{2},$$

for $k = 0, \dots, n$, where $t_{k+1/2} := t_k^*$ is given by (15) and $a_{j,k}, b_{j,k}$ are parameters computed with the conditions $\widetilde{m}_1(t_{k+j/2}) = m_1(t_{k+j/2})$ and $\widetilde{m}_1(t_{k+(j+1)/2}) = m_1(t_{k+(j+1)/2})$. It follows

$$a_{j,k} = \frac{m_1(t_{k+(j+1)/2}) - m_1(t_{k+j/2})}{t_{k+(j+1)/2} - t_{k+j/2}},\ b_{j,k} = m_1(t_{k+j/2}).$$

The key point is that the coefficients $a_{j,k}, b_{j,k}$ depend explicitly on $t_1, \dots, t_n, T$ and can be generated using symbolic computation.
A geometric picture of this construction is given in Fig.2.

4.3 Approximation of F

Using (12), we construct an explicit approximation $\widetilde{F}$ of F using the approximations $\widetilde{m}_1$ and $\widetilde{m}_2$ as follows.

Proposition 4 *Choosing $\widetilde{m}_1$ in $\mathcal{C}_{pe}$ and $\widetilde{m}_2$ as a piecewise constant function on $[0,T]$, the function:*

$$\widetilde{F}(t) = A_0 \int_0^t \widetilde{M}(t)\widetilde{M}^{-1}(s)\,\widetilde{m}_1(s)\,\mathrm{d}s, \qquad (16)$$

where $\widetilde{M}(t) = \exp\left(-\int_0^t \widetilde{m}_2(s)\,\mathrm{d}s\right)$, has a closed-form expression in $\mathcal{C}_{pe}$.

PROOF. Decomposing the integral (16) as a sum of integrals over the partition $(t_{i+j/p})_{ij}$ gives the expression:

$$\widetilde{F}(t)/A_0 = \sum_{i=0}^{k_t-1}\sum_{j=0}^{p-1}\int_{t_{i+j/p}}^{t_{i+(j+1)/p}} \widetilde{M}(t)\widetilde{M}^{-1}(s)\,\widetilde{m}_1(s)\,\mathrm{d}s$$
$$+ \sum_{j=0}^{j_t-1}\int_{t_{k_t+j/p}}^{t_{k_t+(j+1)/p}} \widetilde{M}(t)\widetilde{M}^{-1}(s)\,\widetilde{m}_1(s)\,\mathrm{d}s$$
$$+ \int_{t_{k_t+j_t/p}}^{t} \widetilde{M}(t)\widetilde{M}^{-1}(s)\,\widetilde{m}_1(s)\,\mathrm{d}s, \qquad (17)$$

for $t \in [t_{k_t+j_t/p}, t_{k_t+(j_t+1)/p}]$, $k_t = 0, \dots, n$, $j_t = 0, \dots, p-1$. The term $\widetilde{M}(t)\widetilde{M}^{-1}(s)\widetilde{m}_1(s) = \exp\left(\int_s^t \widetilde{m}_2(u)\,\mathrm{d}u\right)\widetilde{m}_1(s)$ has an explicit expression in $\mathcal{C}_{pe}$ since $\widetilde{m}_2$ is piecewise constant and $\widetilde{m}_1$ is in $\mathcal{C}_{pe}$. Therefore $\widetilde{F}$ has an explicit expression in $\mathcal{C}_{pe}$.

For practical reason, it is important to obtain upper and lower approximations of the force F. The following proposition goes into this direction and is proved in the Appendix.

Proposition 5 *Take $k \in \{0, \dots, n\}$. Assume $\widetilde{m}_2$ is a piecewise constant approximation of m_2 such that $\widetilde{m}_2^k(.;\nu) = \nu\,\overline{m}_2^k(.)$. Then there exists $\nu^+ \geq 1$ (resp. $\nu^- \leq 1$) such that the approximation $\widetilde{F}^+(.;\nu)$ (resp. $\widetilde{F}^-(.;\nu)$), defined by (16) with $\widetilde{m}_2$ is replaced by $\widetilde{m}_2(.;\nu)$, satisfies*

$$\widetilde{F}^+(t_k;\nu) \leq F(t_k) \text{ for all } \nu \geq \nu^+ \geq 1$$

if $0 \leq \widetilde{m}_1 \leq m_1$ on $[0,T]$, and

$$\widetilde{F}^-(t_k;\nu) \geq F(t_k) \text{ for all } \nu \leq \nu^- \leq 1$$

if $0 \leq m_1 \leq \widetilde{m}_1$ on $[0,T]$.

Error estimate. The following proposition gives an upper bound on the error between $\widetilde{F}$ and F and is proved in the Appendix.

Proposition 6 *Assume that $\widetilde{m}_1$ is in $\mathcal{C}_{pe}$ satisfying $0 \leq \widetilde{m}_1(t) \leq 1$ and $\widetilde{m}_2$ is the piecewise constant approximation defined by $\widetilde{m}_2^k = \overline{m}_2^k$ for $k = 0, \dots, n$. Then, the error between the force F and its approximation $\widetilde{F}$ defined by (16) satisfies for $k = 0, \dots, n$:*

$$|F(t_k) - \widetilde{F}(t_k)|/A_0 \leq \int_0^{t_k} |m_1(s) - \widetilde{m}_1(s)|\,\mathrm{d}s$$
$$+ t_k \int_0^{t_k} |m_2(s) - \widetilde{m}_2(s)|\,\mathrm{d}s.$$

5 Numerical results

5.1 Functional specification for the computation of a pulses train

The aim is to compute a local minimum $\sigma^* = (\eta_0^*, \ldots, \eta_n^*, t_1^*, \ldots, t_n^*, T) \in \mathbb{R}_+^{2n+2}$ of a cost function denoted as Θ depending on the training program we have chosen. The *free final time* T adjusts automatically the optimal frequency of the pulses train. The functional specification of the electrostimulator imposes efficient computation of this minimum (real time computation) and this prevents us (at least when Θ involves the force) from using direct or indirect methods such as those presented in Bakir et al. (2020), mainly because these methods are based on a numerical integration scheme to approximate the variable F.

Our numerical scheme presented in this section first generates using symbolic computations the explicit expression of an approximation of Θ denoted as $\widetilde{\Theta}$ in terms of the optimization variables η_i, t_i. This expression can be computed offline and constitutes the objective function of the optimization routine.

5.2 Finite dimensional optimization methods

We recall basic facts about finite dimensional optimization, see Boyd et al. (2004) for details, to emphasize that an optimal sampled-data control problem can be viewed as an instance of such optimization problem.

The optimization problems, associated to the optimal sampled-data control problems **OCP1** and **OCP2** presented in Section 3.2, can be written in the form:

$$\min_{\sigma} \Theta(\sigma), \qquad \Im(\sigma) \leq 0, \tag{18}$$

where $\Im(\sigma) = (\Xi_1(\sigma), \ldots, \Xi_{3n+5}(\sigma))$ is the vector of constraints defined by:

$$\begin{aligned}
&\Xi_i(\sigma^*) = t_{i-1}^* - t_i^* + I_{\min},\ i = 1, \ldots, n,\\
&\Xi_{n+1}(\sigma^*) = t_n^* - T,\\
&\Xi_{n+2+i}(\sigma^*) = -\eta_i^*,\ i = 0, \ldots, n+1,\\
&\Xi_{2n+4+i}(\sigma^*) = \eta_i^* - 1,\ i = 0, \ldots, n+1.
\end{aligned}$$

The cost $\Theta : \sigma \mapsto \Theta(\sigma)$ is related to the endurance or the force strengthening program and is smooth with respect to σ (see Proposition 2).
Consider the Lagrangian defined for all $(\sigma, \mu) \in \mathbb{R}^{2n+1} \times \mathbb{R}_+^{3n+5}$ by:

$$\mathcal{L}(\sigma, \mu) \coloneqq \Theta(\sigma) + \mu \cdot \Im(\sigma).$$

The problem (18) can be written as

$$\inf_{\sigma \in \mathbb{R}^{2n+1}} \sup_{\mu \in \mathbb{R}_+^{3n+5}} \mathcal{L}(\sigma, \mu)$$

and its dual as $\sup_{\mu \in \mathbb{R}_+^{3n+5}} \inf_{\sigma \in \mathbb{R}^{2n+1}} \mathcal{L}(\sigma, \mu)$. First order necessary optimality conditions for σ^* to be a local minimizer state that there exists a Lagrange multiplier $\lambda \in \mathbb{R}^{3n+5}$ such that

$$\begin{aligned}
&\nabla_\sigma \mathcal{L}(\sigma^*, \lambda) = 0,\ \lambda_i \Xi_i(\sigma^*) = 0\\
&\lambda_i \geq 0,\ \Xi_i(\sigma^*) \leq 0,\ i = 1, \ldots, 3n+5.
\end{aligned}$$

We usually do not solve directly these optimality conditions to compute an primal-dual pair (σ^*, λ), but a relaxation of these conditions can lead to efficient algorithm, namely the primal-dual interior point method Boyd et al. (2004).

5.3 Force optimization

We consider the endurance and force strengthening optimization problems **OCP1** and **OCP2**. For each problem, we give the approximation $\widetilde{\Theta}$ of the cost functions Θ based on the approximation $\widetilde{F}$ of the variable F described in section 4. We solve the associated problem (18) – where Θ is replaced by its approximation $\widetilde{\Theta}$ – using an interior point method on a standard computer [1]. Note that $\widetilde{\Theta}$ may consist of million of bytes, for that reason we compute an approximation of the gradient of $\widetilde{\Theta}$ with respect to $t_i,\ i = 1, \ldots, n$ using finite differences (although formal computation of the gradient of $\widetilde{\Theta}$ may be carried out offline). We initialize the pulses train to a regular partition of $[0, 1]$ and the initial amplitudes to 1.

The force approximation $\widetilde{F}$ is defined by (16) and the piecewise affine functions $\widetilde{m}_1, \widetilde{m}_2$ are taken to be equal on $[t_k, t_{k+1}]$, $k = 0, \ldots, n$ to:

$$\begin{aligned}
\widetilde{m}_1(t) &= \begin{cases} m_1(t_{k+1/2}) & \text{if } t \in [t_k, t_{k+1/2}] \\ a_{1j,k}\,(t - t_{k+1}) + b_{1j,k}, & \text{if } t \in [t_{k+1/2}, t_{k+1}] \end{cases},\\
\widetilde{m}_2(t) &= \begin{cases} \frac{m_2(t_k) + m_2(t_{k+1/2})}{2} & \text{if } t \in [t_k, t_{k+1/2}] \\ \frac{m_2(t_{k+1/2}) + m_2(t_{k+1})}{2}, & \text{if } t \in [t_{k+1/2}, t_{k+1}] \end{cases},
\end{aligned} \tag{19}$$

where $t_{k+1/2} = \underset{u \in [t_k, t_{k+1}]}{\operatorname{argmax}} c_N(u)$, $a_{1j,k} = (m_1(t_{k+1}) - m_1(t_{k+1/2}))/(t_{k+1} - t_{k+1/2})$ and $b_{1j,k} = m_1(t_{k+1})$.

5.3.1 Problem OCP1.

The objective function $\Theta(\sigma) = -F(T)$ is approximated by the function $\widetilde{\Theta}(\sigma) = -\widetilde{F}(T)$. The optimization varia-

[1] 4 Intel@Core^{TM} i5 CPU @ 2.4Ghz

bles consist in the impulse times while the amplitudes are fixed to 1.

Numerical result: The optimal solution σ^*, the force response F and its approximation $\widetilde{F}$ are depicted in Fig.3.

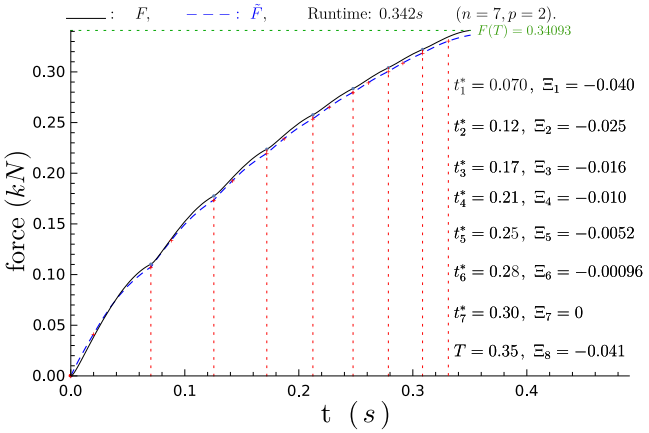

Fig. 3. The optimal solution $\sigma^* = (t_1^*, \ldots, t_n^*, T)$ minimizes the cost $\Theta(\sigma) = \max_\sigma \widetilde{F}(T)$ (T free) (see (16) for the definition of $\widetilde{F}$) under the constraints $\Xi_i \leq 0,\ i = 1, \ldots, n+1$ (see (18)). The continuous curve is the response $t \mapsto F(t)$ to σ^*. Values of the constants are $\tau_c = 20$ms, $n = 7$, $I_{\min} = 20$ms.

5.3.2 Problem OCP2.

The cost $\Theta(\sigma) = \displaystyle\int_0^T |F(s) - F_{ref}|^2 \, \mathrm{d}s$ is approximated by:

$$\widetilde{\Theta}(\sigma) = \sum_{k=0}^{n} \left(\widetilde{F}^+(t_{k+1}; \nu) - F_{ref}\right)^2 (t_{k+1} - t_k),$$

where the upper approximation $\widetilde{F}^+(.;\nu)$ (introduced in Proposition 5) is defined from $\widetilde{m}_1$ given by (19) and $\widetilde{m}_2(.;\nu)$ given by

$$\widetilde{m}_2^k(t;\nu) = \nu \begin{cases} \frac{m_2(t_k)+m_2(t_{k+1/2})}{2} & \text{if } t \in [t_k, t_{k+1/2}] \\ \frac{m_2(t_{k+1/2})+m_2(t_{k+1})}{2}, & \text{if } t \in [t_{k+1/2}, t_{k+1}] \end{cases}.$$

Numerical result: The optimal solution σ^*, the force response F and its upper approximation $\widetilde{F}^+(.;\nu = 0.8)$ are depicted in Fig.4. We also represent the lower approximation $\widetilde{F}^-(.;\nu = 1.1)$, which is the response force for the input σ^*.

6 Isometric case: design of a smart muscular electrostimulator

In this section we apply our study in the isometric case associated to the conception of a smart electrostimulator. In this case, the task is to assign a reference

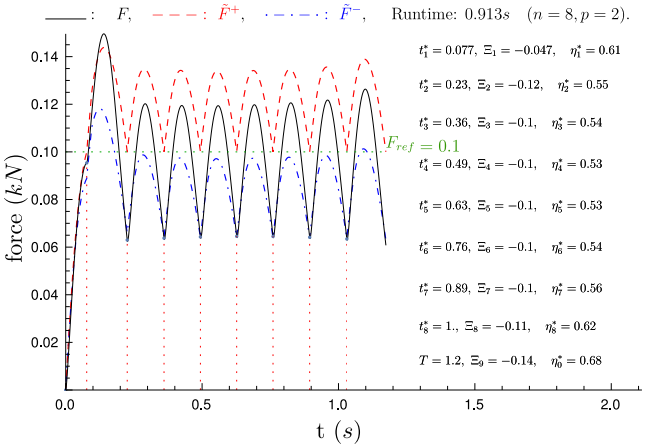

Fig. 4. The optimal solution $\sigma^* = (\eta_0^*, \ldots, \eta_n^*, t_1^*, \ldots, t_n^*, T)$ minimizes the cost $\min_\sigma \sum_{k=0}^n \left(\widetilde{F}^+(t_{k+1}; \nu{=}0.8) - F_{ref}\right)^2 (t_{k+1} - t_k)$ ($T = t_{n+1}$ is free), where $\widetilde{F}^+(.;\nu{=}0.8)$ is the upper approximation of F (see Proposition 5) represented by the dashed curve under the constraints $\Xi_i \leq 0,\ i = 1, \ldots, 3n+5$ (see (18)). The continuous curve is the response $t \mapsto F(t)$ to σ^* and the dash-dotted curve is the lower approximation $\widetilde{F}^-(.;\nu{=}1.1)$ associated to σ^*). Values of the constants are $\tau_c = 20$ms, $n = 8$, $I_{\min} = 20$ms and $F_{ref} = 0.1$kN.

force, but the general frame is suboptimal motion planning, see Hirschorn et al. (1987, 1988) for the theoretical foundations.

Advanced commercial muscular electrostimulator for training or reeducation purposes are based on the following. First of all, the user defines a program training. Basically it is an endurance program with low frequency sequences of trains (with constant interpulse) or a force strengthening program with high frequency trains. The program is a sequence of trains or rest periods. Before starting, the muscle is scanned to determine the parameters. A smart electrostimulator based on our study aims to design automatically such sequence, each program being translated into an optimization problem. Besides, in our framework, one can use VFT (Variable Frequency Trains) vs CFT (Constant Frequency Trains) in the standard case to complete the tuning of the amplitude.

We illustrate the implementation of the endurance program in the smart electrostimulator (see Fig.5) associated to optimization program OCP2 defined in Section 3.2.2.

(1) First we estimate, using the methods proposed in Stein et al. (2013); Wilson (2011), the parameters $\overline{R}, \tau_{1,0}, K_{m,0}, \tau_2, \tau_c, A_0, \alpha_A, \tau_{fat}$ of the reduced force-fatigue model.
(2) Once the model is calibrated, we compute the maximal muscle strength F_{tet}, which is the asymptotic force response to a high frequency train over $[0, T]$.
(3) This allows to fix a reference force $F_{ref} = F_{tet}/\rho$,

where $\rho > 1$ and we compute the input σ^* minimizing $\int_0^T |\widetilde{F}(s) - F_{ref}|^2 \, ds$ over σ (see Section 5).

(4) We apply the train pulses defined by σ^* and we come back to instruction (1).

The muscle fatigue effect is taken into account by reducing the reference force F_{ref} during the training period and is related to new estimation of the fatigue.

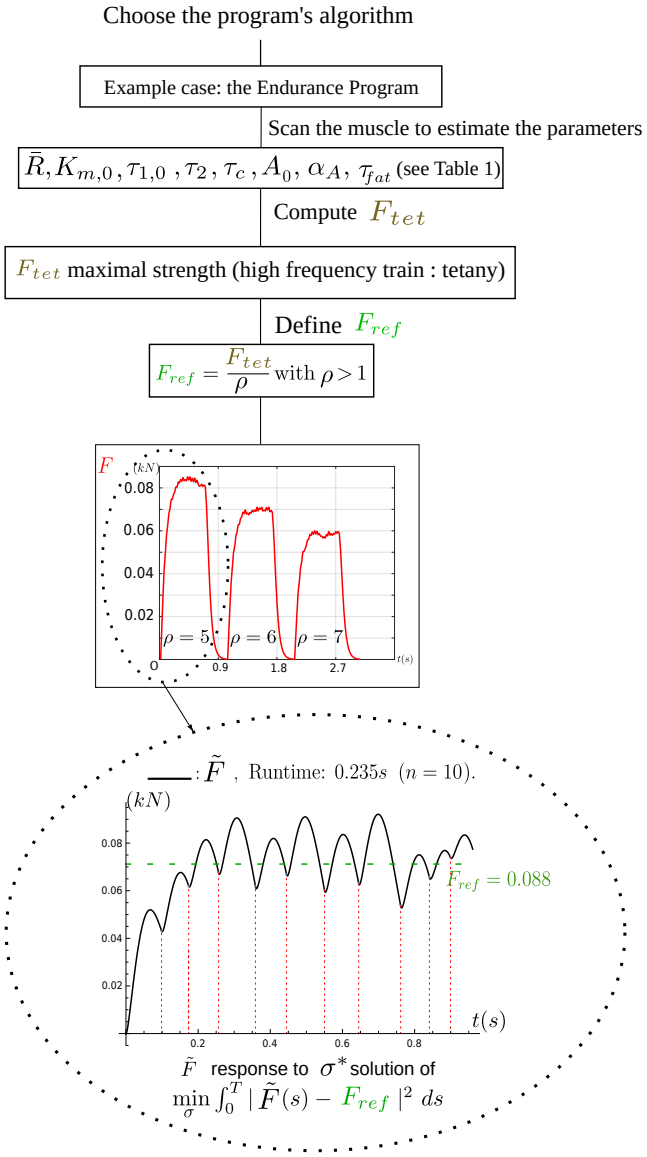

Fig. 5. Illustration of the endurance program for a smart electrostimulator.

7 Conclusion

In this short article, we have mainly constructed a finite dimensional approximation of the muscular force response to FES-input exploiting the mathematical structure of the model. The construction is based on the Ding et al. model but can be adapted to deal with the different models discussed in Wilson (2011). We have presented one application of our study in the isometric case in view to design a smart electrostimulator, which is an ongoing industrial project. Our approximation can be used to parameters estimation Stein et al. (2013); Wilson (2011) and to design MPC-optimized sampled-data control schemes, applying standard algorithms Richalet (1993); Wang et al. (2010) to this situation.
Another application of our study is to track in the non-isometric case a path in the joint angle variable and this will be developed in a forthcoming article.

Acknowledgements

The authors thank Mokrane Abdiche for his involvement in the project, as well as Segula Matra Automotive and French Association Nationale de la Recherche et de la Technologie (ANRT) for their financial support.

References

Ambrosio L., Da Prato G. & Mennucci A. (2011). Introduction to Measure Theory and Integration. Appunti/Lecture Notes, 187 pages.

Bakir T., Bonnard B. & Rouot J. (2019). A case study of optimal input-output system with sampled-data control: Ding et al. force and fatigue muscular control model. *Netw. Hetero. Media*, **14**(1) 79–100.

Bakir T., Bonnard B., Bourdin L. & Rouot J. (2020). Pontryagin-type conditions for optimal muscular force response to functional electrical stimulations. *J. Optim. Theory Appl.*, **184** 581–602.

Bonnard B. & Rouot J. (2021). Geometric optimal techniques to control the muscular force response to functional electrical stimulation using a non-isometric force-fatigue model. *J. Geom. Mech., American Institute of Mathematical Sciences (AIMS)*, **13**(1), 1–23.

Bourdin L. & Trélat E. (2016). Optimal sampled-data control, and generalizations on time scales. *Math. Cont. Related Fields*, **6**, 53–94.

Boyd S. & Vandenberghe L. (2004). Convex Optimization. *Cambridge, U.K.: Cambridge Univ. Press.*, 716 pages.

Doll B.D. , Kirsch N.A. & Sharma N. (2015). Optimization of a Stimulation Train based on a Predictive Model of Muscle Force and Fatigue. *IFAC-PapersOnLine*, **48**(20), 338–342.

Ding J., Wexler A.S. & Binder-Macleod S.A. (2000). Development of a mathematical model that predicts optimal muscle activation patterns by using brief trains. *J. Appl. Physiol.*, **88** 917–925.

Ding J., Wexler A.S. & Binder-Macleod S.A. (2002a). A predictive fatigue model. I. Predicting the effect of stimulation frequency and pattern on fatigue. IEEE Transactions on Neural Systems and Rehabilitation Engineering, **10**(1), 48–58.

Ding J., Wexler A.S. & Binder-Macleod S.A. (2002b). A predictive fatigue model. II. Predicting the effect of resting times on fatigue. IEEE Transactions on Neural Systems and Rehabilitation Engineering, **10**(1) 59–67.

Gesztelyi R., Zsuga J., Kemeny-Beke A., Varga B., Juhasz B. & Tosaki A.. (2012). The Hill equation and the origin of quantitative pharmacology. *Archive for history of exact sciences* 66(4) 427–438.

Hirschorn R. M. & Davis J. H. (1987). Output tracking for nonlinear systems with singular points. SIAM J. Control Optim. **25**(3) 547–557.

Hirschorn R. M. & Davis J. H. (1988). Global output tracking for nonlinear systems. SIAM J. Control Optim. 26(6) 1321–1330.

Isidori A. (1995). Nonlinear Control Systems. *3rd ed. Berlin, Germany: Springer-Verlag*, 549 pages.

Marion M.S., Wexler A.S. & Hull M.L. (2013). Predicting non-isometric fatigue induced by electrical stimulation pulse trains as a function of pulse duration. *Journal of neuroengineering and rehabilitation*, **10**(13).

Michaelis L. & Menten M.L. (1913). Die Kinetik der Intertinwerkung. *Biochemische Zeitschrift*, **49** 333-369.

Richalet J. (1993). Industrial applications of model based predictive control. *Automatica, IFAC* **29**(5) 1251–1274.

Stein R., Bucci V., Toussaint N.C., Buffie C.G., Rätsch G., Pamer E.G. et al. (2013). Ecological Modeling from Time-Series Inference: Insight into Dynamics and Stability of Intestinal Microbiota. *PLOS Computational Biology* **9**(12) 1–11.

Wang Y. & Boyd S. (2010). Fast Model Predictive Control using Online Optimization. *IEEE Transactions on Control Systems Technology*. **18**(2) 267–278.

Wilson E. (2011). Force response of locust skeletal muscle. Southampton University, Ph.D. thesis.

Toufik Bakir. Toufik Bakir received his Ph.D. degree in industrial automatics from the University of Claude Bernard-Lyon I, Lyon, France, in 2006. He was associate professor with the university of Burgundy (2007-2020). He became full professor since 2021 at ImViA (Image and Artificial Vision laboratory) in the University of Burgundy. His research interests include dynamical systems, systems modeling, optimization, and control.

Bernard Bonnard. Ph.D. degree in Mathematics, 1978 University of Metz and Thèse d'État ès Sciences, 1983, INPG and University of Grenoble. Postdoctoral positions: Control Theory Center, University of Warwick and Division Applied Sciences Harvard University. Permanent CNRS researcher from 1979 to 1991. Professor University of Burgundy, Institut de Mathématiques de Bourgogne, since 1991 and INRIA Sophia Antipolis researcher since 2011 (McTAO Team). Author of four books in Optimal Control and more than 130 research articles in optimal control, dynamical systems and geometry with applications to space mechanics, quantum control, magnetic resonance imaging, biomedical models (microswimmers, generalized Lotka-Volterra equations and microbiote, Hill–Huxley model in biomechanics).

Sandrine Gayrard. She received an engineer's degree from Ense3 – Grenoble INP in 2020 and since 2020, she is preparing a thesis in control engineering through a CIFRE (Industrial Agreements for Training through Research) contract between University of Burgundy and Segula Matra Automotive under the supervision of T. Bakir and B. Bonnard.

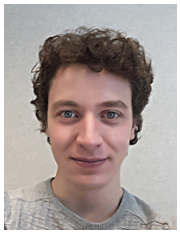

Jérémy Rouot. Ph.D. degree in Mathematics in 2016 from University Nice Côte d'Azur for its works in Optimal Control motivated by microswimming and space mechanics applications. In 2017, he worked as a postdoc in LAAS-CNRS (Toulouse) on the inverse optimal control problem. From 2017 to 2021, he was lecturer and researcher in two engineering schools EPF (Troyes) and ISEN (Brest) and he became assistant professor in 2021 from the University of Western Brittany, LMBA (Brest) working on non smooth optimal control, optimal synthesis with applications to chemical reactors and mathematical biology.

Appendix

This appendix give the proofs of the propositions 5 and 6.

Using (12)-(16), we can compute $F(t_k) - \widetilde{F}(t_k),\ k \in \{0, \dots, n\}$ as follows:

$$\begin{aligned}(F(t_k) - \widetilde{F}(t_k))/A &= \int_0^{t_k} M(t_k)M^{-1}(s)m_1(s) - \widetilde{M}(t_k)\widetilde{M}^{-1}(s)\widetilde{m}_1(s)\,\mathrm{d}s \\ &= \int_0^{t_k} M(t_k)M^{-1}(s)(m_1(s) - \widetilde{m}_1(s))\,\mathrm{d}s + \int_0^{t_k} (M(t_k)M^{-1}(s) - \widetilde{M}(t_k)\widetilde{M}^{-1}(s))\widetilde{m}_1(s)\,\mathrm{d}s \\ &= \int_0^{t_k} (m_1(s) - \widetilde{m}_1(s))\,\mathrm{d}s + \int_0^{t_k} \left(\exp\left(-\int_s^{t_k} m_2(u)\,\mathrm{d}u\right) - \exp\left(-\int_s^{t_k} \widetilde{m}_2(u)\,\mathrm{d}u\right)\right)\widetilde{m}_1(s)\,\mathrm{d}s.\end{aligned} \tag{20}$$

Proof of Proposition 5. Assume the approximation $\widetilde{F}$ is constructed from the piecewise approximations $\widetilde{m}_1, \widetilde{m}_2$ satisfying $\widetilde{m}_1 \geq 0$ and for all $k \in \{0, \dots, n\}$: $\widetilde{m}_2^k = \nu\,\overline{m}_2^k$, where $\nu \in \mathbb{R}$ is a parameter.

With these conditions, we rewrite the last integral term of (20) as

$$\begin{aligned}&\int_0^{t_k} \left(\exp\left(-\int_s^{t_k} m_2(u)\,\mathrm{d}u\right) - \exp\left(-\int_s^{t_k} \widetilde{m}_2(u)\,\mathrm{d}u\right)\right)\widetilde{m}_1(s)\,\mathrm{d}s \\ &= \sum_{i=0}^{k-1} \exp\left(-\sum_{j=i+1}^{k-1}(t_{j+1} - t_j)\overline{m}_2^j\right)\int_{t_i}^{t_{i+1}} \exp\left(-\int_s^{t_{i+1}} m_2^i(u)\,\mathrm{d}u\right) \\ &\left(1 - \exp\left(-\sum_{j=i+1}^{k-1}(t_{j+1} - t_j)\overline{m}_2^j(\nu - 1)\right)\exp\left(\int_s^{t_{i+1}} m_2^i(u)\,\mathrm{d}u - \nu\int_s^{t_{i+1}} \widetilde{m}_2^i(u)\mathrm{d}u\right)\right)\widetilde{m}_1(s)\,\mathrm{d}s.\end{aligned} \tag{21}$$

Clearly, if $\widetilde{m}_1 \leq m_1$ there exists $\nu^+ \geq 1$ large enough such that for all $\nu \geq \nu^+$, $F(t_k) \geq \widetilde{F}(t_k)$. Likewise, if $\widetilde{m}_1 \geq m_1$ there exists $\nu^- \leq 1$ small enough such that for all $\nu \leq \nu^-$, $F(t_k) \leq \widetilde{F}(t_k)$. □

Proof of Proposition 6. Here we assume that the approximations $\widetilde{m}_1, \widetilde{m}_2$ satisfy

$$0 \leq \widetilde{m}_1^k \leq m_1^k \leq 1 \ \text{ and } \ 0 \leq \widetilde{m}_2^k = \overline{m}_2^k \ \text{ on } [t_k, t_{k+1}], \text{ for all } k \in \{0, \dots, n\}.$$

From (20), we can write

$$\begin{aligned}|F(t_k) - \widetilde{F}(t_k)|/A &\leq \int_0^{t_k} |m_1(s) - \widetilde{m}_1(s)|\,\mathrm{d}s + \int_0^{t_k} \left|\exp\left(-\int_s^{t_k} m_2(u)\,\mathrm{d}u\right) - \exp\left(-\int_s^{t_k} \widetilde{m}_2(u)\,\mathrm{d}u\right)\right|\,\mathrm{d}s \\ &\leq \int_0^{t_k} |m_1(s) - \widetilde{m}_1(s)|\,\mathrm{d}s + \int_0^{t_k}\int_s^{t_k} |m_2(u) - \widetilde{m}_2(u)|\,\mathrm{d}u\,\mathrm{d}s \\ &\qquad\qquad \text{(by Lipschitz continuity of } \exp \text{ on } [a, 0], a < 0) \\ &\leq \int_0^{t_k} |m_1(s) - \widetilde{m}_1(s)|\,\mathrm{d}s + t_k\int_0^{t_k} |m_2(u) - \widetilde{m}_2(u)|\,\mathrm{d}u,\end{aligned}$$

which yields the expected result. □